

## EBSD Study of Substructure and Texture Formation in Dual-Phase Steel Sheets for Semi-Finished Products

M. Masimov<sup>1, a</sup>, N. Peranio<sup>2, b</sup>, B. Springub<sup>1, c</sup>, F. Roters<sup>2, d</sup> and D. Raabe<sup>2, e</sup>

<sup>1</sup>Salzgitter Mannesmann Forschung GmbH, Eisenhüttenstrasse 99, 38239 Salzgitter, Germany

<sup>2</sup>Max-Planck-Institute for Iron Research GmbH, Max-Planck-Strasse 1, 40237 Düsseldorf, Germany

<sup>a</sup> m.masimov@sz.szmf.de, <sup>b</sup> n.peranio@mpie.de, <sup>c</sup> b.springub@sz.szmf.de, <sup>d</sup> f.roters@mpie.de, <sup>e</sup> d.raabe@mpie.de

**Keywords:** dual phase steels, orientation imaging microscopy, rolling, annealing, texture, EBSD

**Abstract.** Using SEM/EBSD the substructure and texture evolution in dual phase steels in the first steps of the process chain, i.e. hot rolling, cold rolling, and following annealing were characterized. In order to obtain dual phase steels with high ductility and high tensile strength an industrial process was reproduced by cold rolling of industrially hot rolled steel sheets of a thickness of 3.75 mm with ferrite and pearlite morphology down to a thickness of 1.75 mm and finally annealing at different temperatures. Such technique allows a compilation of ferrite and martensite morphology typical for dual phase steels. Due to the competition between recovery, recrystallization and phase transformation during annealing a variety of ferrite martensite morphologies was produced by promoting one of the mechanisms through the variation of technological parameters such as heating rate, intercritical annealing temperature, annealing time, cooling rate and the final annealing temperature. Annealing induced changes of the mechanical properties were determined by hardness measurements and are discussed on the basis of the results of the substructure investigations.

### Introduction

A cost reduction can be achieved by an optimization of the entire production process. For this, an integral simulation concept was elaborated for reducing the entire expensive experimental process chain [1]. This concept comprises areas such as crystal plasticity for cold rolling, cellular automata for microstructure evolution during thermal treatment, continuum mechanics for deep drawing, and crash simulation. The contribution presented here is a part of a project supported by the German Ministry of Education and Research and is devoted to the analysis of the first steps of the process chain, i.e., the microstructure and texture evolution in hot rolled, cold rolled and annealed sheets of dual-phase steels.

### Experimental

#### *Materials*

The starting material was hot rolled steel with a chemical composition consisting of 0.147 wt. % C, 1.9 wt. % Mn, 0.4 wt. % Si. The steel sheets with a thickness of 3.75 mm consisting of about 65% ferrite and 35% pearlite were industrially cold rolled down to a thickness of 1.75 mm and annealed at an intercritical annealing temperature. Further the samples were annealed at temperatures slightly below the martensite start temperature [2].

#### *Measurements*

Structural and texture analyses were carried out by field emission scanning electron microscopy (SEM, Jeol JSM 6500 F) combined with electron backscatter diffraction (EBSD). The samples of transverse and longitudinal sections were prepared by a procedure including grinding, mechanical polishing and etching. For EBSD measurements the samples were additionally polished with a suspension of 0.1 µm-diameter silica particles. EBSD measurements were carried out by using a DigiView detector at an accelerating voltage of 15 kV. A measurement area of 80x200 µm<sup>2</sup> with a

step size of 0.2  $\mu\text{m}$  in the center and at the surface of transverse and longitudinal sections of the sheets was used for substructure analysis. The texture analysis was carried out in a measurement area extending from the center ( $t = 0$ ) to the surface ( $t = 1$ ) of the sheets with a width of 700  $\mu\text{m}$  in transverse direction (TD) and a length of 1000  $\mu\text{m}$  in normal direction (ND). The measured data were cleaned up by a single iteration and grain dilation using a grain tolerance angle of  $5^\circ$  and a minimum grain size of 5 measurement points.

The structural analysis and determination of structural constituents in dual phase steels was carried out by using the following EBSD based measures:

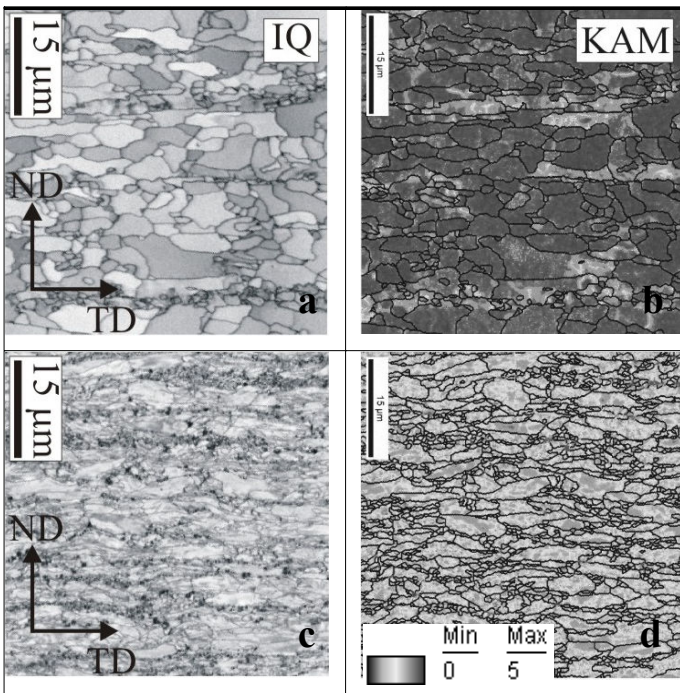
- Image Quality (IQ) – a measure for the diffuse character of the Kikuchi diffraction patterns [3];
- Kernel Average Misorientation (KAM) – average misorientation between a point and all of its neighbors within a certain radius (400 nm) and tolerance value ( $5^\circ$ ) [3].

## Results and Discussions

### Substructure

#### Hot and cold rolled sheets

In SEM images hot rolled sheet revealed a heterogeneously distributed pearlite-ferrite structure with a pearlite fraction of about 35 %. The grain size of pre-eutectoid ferrite was found to be about 5  $\mu\text{m}$ . In the center of the cold rolled sheets, the ferrite and pearlite bandwidths decreased with decreasing sheet thickness. The ferrite grains were extended in normal direction and elongated in rolling direction with decreasing sheet thickness [2]. The IQ and KAM maps, obtained by EBSD, reveal the substructure development in hot rolled steels due to cold rolling (Fig.1). Thus, the high IQ number



(predominantly light gray scales in the IQ maps) and low KAM values (dark areas in the KAM maps) show that density of both statistically distributed dislocations and geometrically necessary dislocations in hot rolled steels are quite low. A cold rolling of sheets leads to formation of inhomogeneous pan-cake substructure with high lattice distortion. The lower values of IQ number and higher KAM values confirm both high densities of randomly distributed dislocations and excess dislocations caused by deformation.

**Figure 1:** Image Quality (a, c) and Kernel Average Misorientation (b, d) maps, obtained by EBSD on hot rolled (a, c), cold rolled (b, d) steels

Figure 2 illustrates the distributions of the image quality number of the hot rolled steels, obtained from the samples center and surface. A similar and narrow IQ distribution for hot rolled steel indicates the homogeneous distribution of lattice strain in the center and surface of samples. Cold rolling broadens the distribution due to strain inhomogeneity caused by statistically distributed dislocations. However, due to different degrees of lattice distortions the IQ distribution, obtained from the sample center is marginal wider than the one for the sample surface (Fig. 2). A comparison of the spatial distribution of misorientations between identified grain boundaries of hot rolled and cold rolled steels is presented in Fig. 2 and the differences between them are obvious. The hot rolled sheet depicts distributions, which are close to random (Mackenzie) distribution indicating marginal

correlations between boundaries. In the case of cold rolling the fraction of the low angle boundaries, related to geometrically necessary dislocations increases and the fraction of high angle boundaries simultaneously decreases. The misorientation distribution, obtained from the surface and center of the sheets for both hot rolled and cold rolled sheets show very small differences.

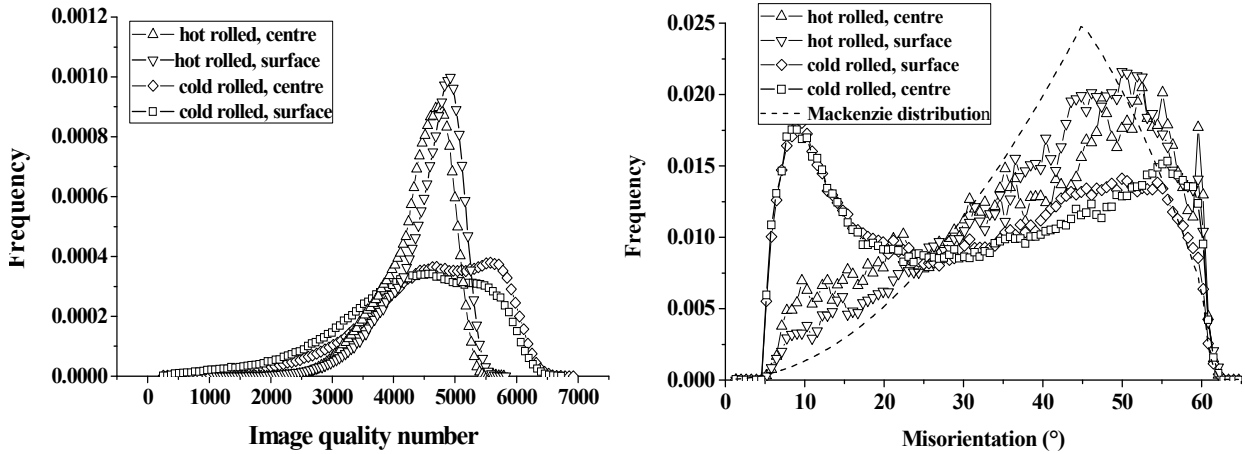


**Figure 2:** Image Quality (a) and spatial misorientation (b) distribution in hot and cold rolled steels

#### Annealed sheets

As known, annealing of cold rolled sheets at an intercritical annealing temperature of 695 °C firstly results in recovery and further in recrystallization. Figure 3 presents the distribution of image quality number of sheets, annealed at temperatures of 695 °C. A decrease in the widths of IQ distribution related to lattice distortions with time can be noticed. The IQ distribution becomes more homogeneous with annealing time. The misorientations in steel sheets, annealed at a temperature of 695 °C, show an identical distribution. But, the fractions of low angle boundaries decrease with the annealing time and the misorientation distributions become similar to the random distribution due to nucleation and growth of new grains.

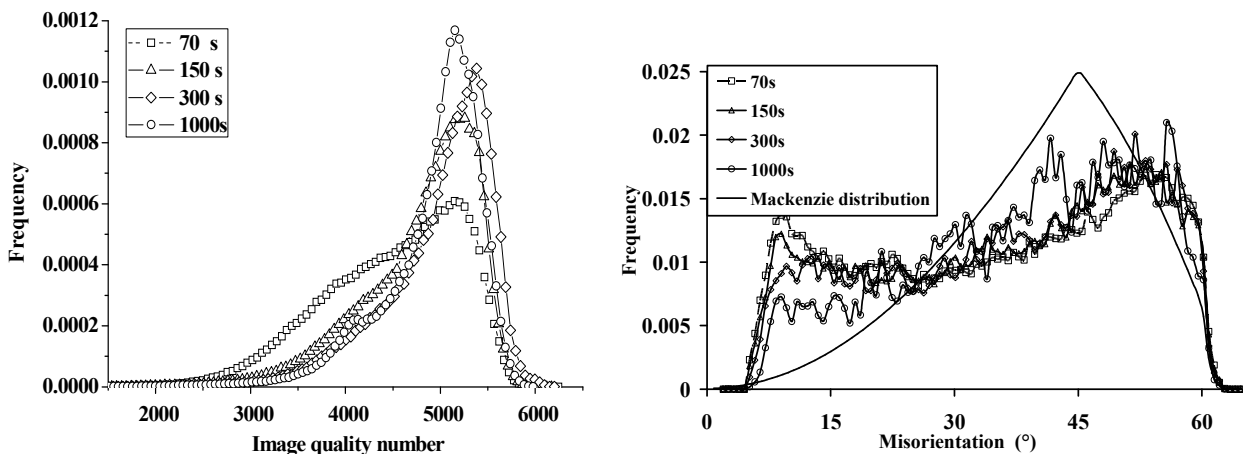


**Figure 3:** IQ distributions (a) and misorientation distributions (b) in samples annealed at a temperature of 695 °C

However, the high frequency of misorientations between neighboring grains at low angles (<15°) remains despite a long annealing time of 1000 s, indicating that the annealing time was not enough for complete recrystallization. The evolution of the lattice strain during the annealing as well as the  $\alpha \rightarrow \gamma$  phase transformation at a temperature of 740 °C can also be studied based on image quality and misorientation angle distributions and is presented in Fig. 4. As seen, starting from an annealing time of 150 s a second small peak with low IQ number appears in on the image quality distribution

corresponding to martensite constituents. The peak becomes more obvious and distinct with increasing of annealing time. The left sides of the IQ distributions were simultaneously shifted to higher numbers, corresponding to undistorted  $\alpha$ -ferrite. Using a fitting and peak deconvolution procedure martensite and ferrite fraction can be quantified, but this task yields reliable results for samples, in which any deformation layer on the samples caused by grinding was fully removed by electrolytic polishing [3].

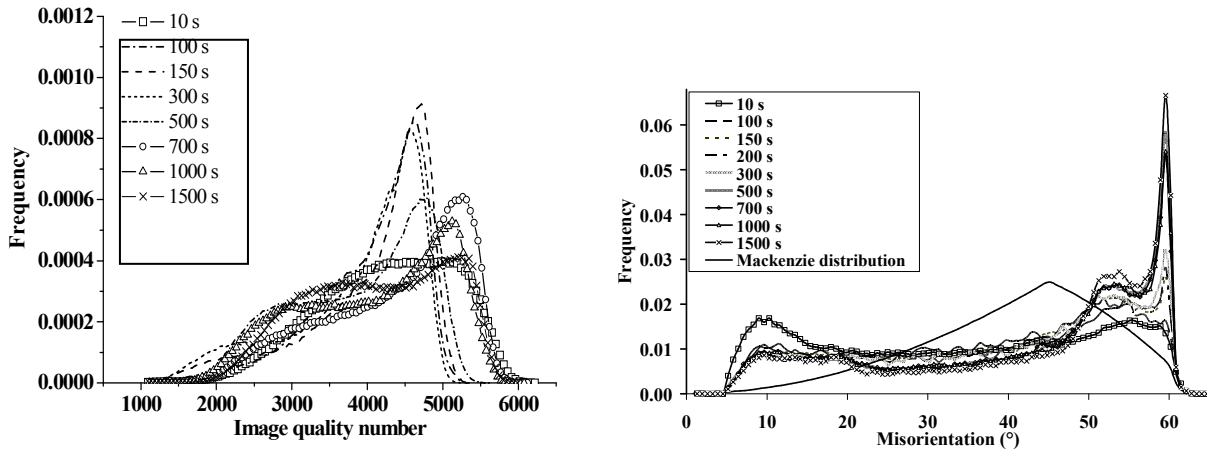


**Figure 4:** IQ distributions and misorientation angle distributions between identified boundaries in samples, annealed at a temperature of 740 °C

The misorientation angle distributions for steel sheets annealed at  $T = 740$  °C presented in Fig. 4 reveals a low frequency of misorientations of  $5^\circ - 50^\circ$  and a high frequency of misorientations of  $53^\circ$  and  $60^\circ$ . Misorientation at  $60^\circ$  is consistent with the misorientations between neighboring grains, bearing Kurdjumov-Sachs relationship with the parent grains (KS/KS). A misorientation of  $53^\circ - 54^\circ$  is due to the misorientations between grains obtained by phase transformations according the relationship of Nishiyama-Wassermann and Kurdjumov-Sachs (NW/KS). The peak at  $60^\circ$  is caused by the axis-angle relationship  $60^\circ\langle 111 \rangle$  (twin-related) and  $60^\circ\langle 110 \rangle$  and corresponds to martensite. A higher frequency of the peaks indicates the higher fraction of martensite constituents. A peak at misorientation angle of  $60^\circ$  firstly occurs at an annealing time of 15 s and its frequency increases with the annealing time confirming ferrite to martensite transformation. Moreover, an annealing of cold rolled steels leads to a decrease in the fraction of low angle boundaries.

### Texture

An overview of the texture inhomogeneity determined by EBSD on a transverse section of the hot rolled sheet is given in Fig. 5 and 6. The fractions of important texture components developed in hot rolling in dependence on the through-thickness position  $t$  are presented in Fig. 6, which is typical for hot rolled steels [6]. Finally, the orientation density  $f(g)$  along characteristic orientation fibers in dependence on the through-thickness position  $t$  is presented in Fig. 6. For the hot rolled sheet presented here, the plane-strain texture in the center of the sheet exhibited a strong  $\alpha$ -fiber and a weak  $\gamma$ -fiber.

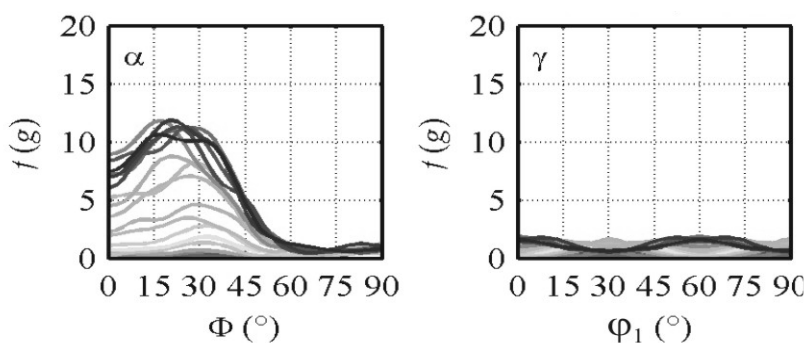


**Figure 5:**  $\alpha$ - and  $\gamma$ -fibers in dependence of the through-thickness position  $t$  ( $t = 0 - 1$ ) in hot rolled steels. Bright fiber lines were obtained in the center ( $t = 0$ ) and dark ones at the surface ( $t = 1$ ) of the sheets.

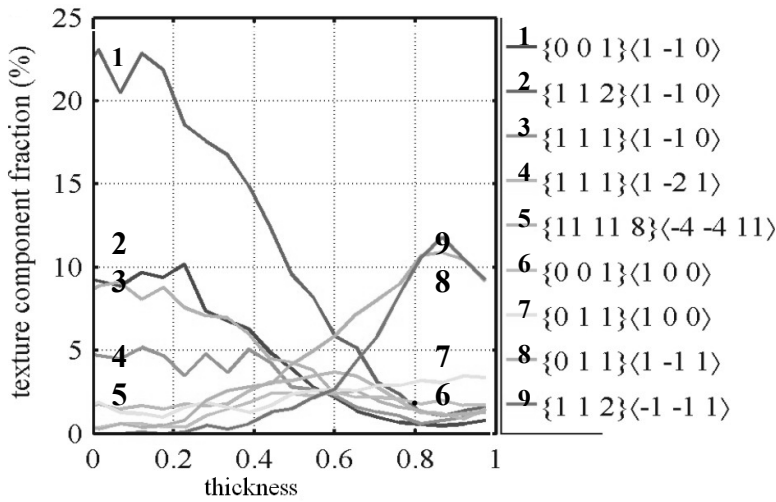


**Figure 6:** Through - thickness texture inhomogeneity in hot rolled sheets: Bright and dark fiber lines were obtained from the center and the surface of the sheets, respectively.

Particularly, the texture component  $\{112\}\langle 110 \rangle$  of  $\alpha$ -fiber shows a strong maximum in the center of the sheet. The dominant features of the shear texture close to the surface of the hot rolled sheets were found to be the texture components  $\{011\}\langle 111 \rangle$  on the  $\alpha$ -fiber and  $\{112\}\langle 111 \rangle$  on the  $\gamma$ -fiber, which both reached their maximum close to the surface of the sheet at  $t = 0.9$ .

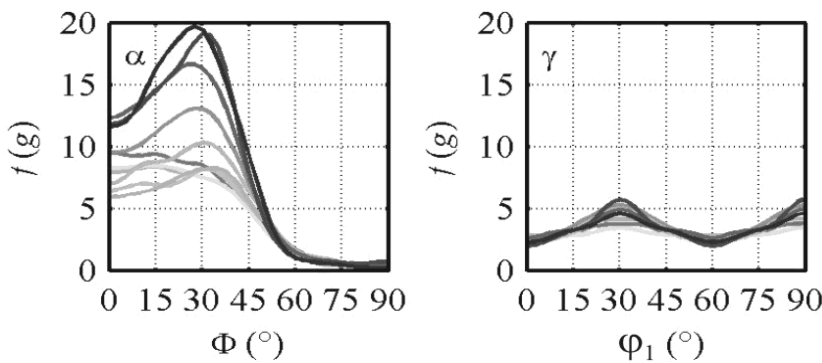


**Figure 7:** Development of  $\alpha$ - and  $\gamma$ -fibers in dependence of the through-thickness position  $t$  ( $t = 0 - 1$ ) in cold rolled steels. Bright fiber lines were obtained in the center ( $t = 0$ ) and dark ones at the surface ( $t = 1$ ) of the sheets.

*Cold rolling* of the steel sheet significantly changed the texture inhomogeneity of the hot rolled sheets. As a result, the through-thickness texture inhomogeneity was reduced and the orientation density of texture components  $\{001\}\langle 1\bar{1}0 \rangle$  and  $\{112\}\langle 1\bar{1}0 \rangle$  of the  $\alpha$ -fiber,  $\{111\}\langle 1\bar{2}1 \rangle$  of the  $\gamma$ -fiber increased (Fig. 7). Particularly, the shear texture at the surface of the sheet was strongly transformed and became more similar to the plane-strain texture in the center of the sheet.

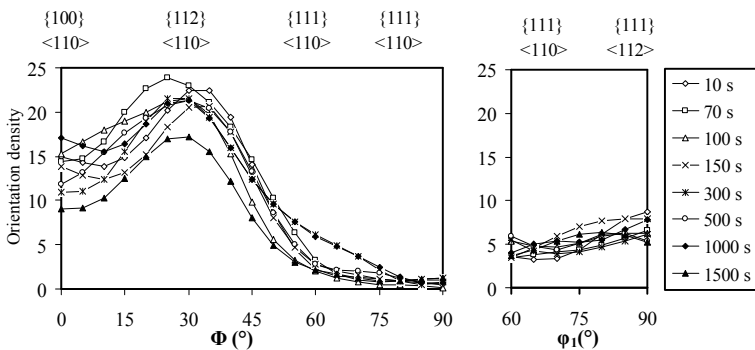


**Figure 8:** Development of  $\alpha$  - and  $\gamma$  -fibers in dependence on the annealing time

*Annealing* of cold rolled samples does not significantly change the rolling texture. The density of strong rolling texture components  $\{112\}\langle 110 \rangle$  and  $\{111\}\langle 112 \rangle$  decreases slightly with the annealing time. Figure 8 illustrates this effect for an annealing temperature of  $740\text{ }^\circ\text{C}$ . Increasing the annealing temperature also results in decreasing the rolling texture components. Figure 9 illustrates the interrelationship between the martensite fraction obtained by SEM and the hardness of steels

obtained for an annealing at a temperature of 740 °C. The hardness of samples firstly decreases due to recovery. Starting from an annealing time of 150 s due to phase transformation and emerging of martensite constituent the hardness increases again. This was also confirmed using the analysis of image quality and misorientations between grain boundaries, as presented in Fig. 4.

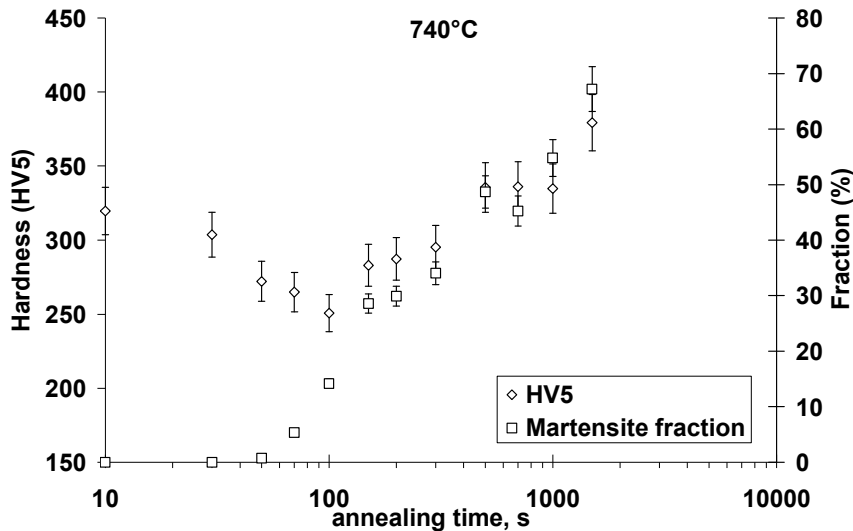


**Figure 9:** Hardness and martensite fraction, obtained in the sheet center vs. annealing time

## Conclusions

In hot rolled sheets, ferrite and pearlite showed a band structure in the center and a heterogeneous distribution at the surface of the sheet. Texture analysis yielded a through-thickness texture inhomogeneity and a maximum plane-strain texture in the center and a maximum shear texture close to the surface of the sheet. Due to cold rolling the in-grain orientation gradients also increased, which is related to an increase of dislocation density and thereby an increase of the driving force for recrystallization. The through-thickness texture inhomogeneity was reduced by cold rolling. Recovery and recrystallization were found to be dominant for annealing at ferritic temperatures and at low intercritical temperatures up to 695 °C. There is an overlap of recrystallization and phase transformation only at intercritical annealing temperatures exceeding 740 °C. A correlation between the volume fraction of martensite and hardness was observed at an intercritical annealing temperature of 740 °C. Increasing the annealing time leads to an increasing martensite fractions and therefore to an increasing hardness.

## Acknowledgments

The authors are grateful to the German Ministry for Education and Research for the financial support of the project under grant no. 03X0501E.

## References

- [1] R. K. Ray: Scripta Metallurgica Vol. 18 (1984), p. 1211
- [2] N. Peanio, F. Roters, D. Raabe, M. Masimov and B. Springub: *submitted to Material Science and Engineering* (2009)
- [3] S. Zaefferer, P. Romano and F. Friedel: J. Microscopy Vol. 230 (2008), p. 499

## **Texture and Anisotropy of Polycrystals III**

doi:10.4028/www.scientific.net/SSP.160

## **EBSD Study of Substructure and Texture Formation in Dual-Phase Steel Sheets for Semi-Finished Products**

doi:10.4028/www.scientific.net/SSP.160.251

### **References**

[1] R. K. Ray: Scripta Metallurgica Vol. 18 (1984), p. 1211

doi:10.1016/0036-9748(84)90107-8

[2] N. Peanio, F. Roters, D. Raabe, M. Masimov and B. Springub: submitted to Material Science and Engineering (2009)

[3] S. Zaefferer, P. Romano and F. Friedel: J. Microscopy Vol. 230 (2008), p. 499

doi:10.1111/j.1365-2818.2008.02010.x

PMid:18503676